Modulation of Indian Summer Monsoon Rainfall response to ENSO in the recent decades and its large-scale dynamics

Tanu Sharma
India Meteorological Department
Satyaban B. Ratna (satyaban14@gmail.com)
India Meteorological Department
D. S. Pai
The Institute for Climate Change Studies (ICCS)

Research Article

Keywords: Indian Summer Monsoon Rainfall, El Niño, La Niña, Pacific Ocean, ENSO-ISMR, Teleconnection

Posted Date: January 3rd, 2023

DOI: https://doi.org/10.21203/rs.3.rs-2405719/v1

Abstract

The El Niño-Southern Oscillation (ENSO) is one of the major drivers of prominent ocean-atmosphere coupled phenomenon over the equatorial Pacific Ocean that strongly modulates the interannual variability of Indian summer monsoon rainfall (ISMR). However, the relationship between ENSO-ISMR has gone through secular variation during different decades. This study comprises a detailed analysis of the changing relationship between the ENSO and ISMR during two recent independent 30-year periods; (i) 1961–1990 and (ii) 1991–2020, using Sea Surface Temperature (SST), rainfall and various atmospheric variables. It was observed that the negative correlation of ENSO with ISMR has significantly weakened during 1991–2020 compared to 1961–1990. It was found that the La Niña associated positive rainfall intensity over central India was reduced during 1991–2020 due to weakening of vertical wind shear as compared to 1961–1990. Similarly, the El Niño associated negative rainfall intensity was reduced over large parts of north and central India during 1991–2020 due to weaker subsidence anomaly compared to 1961–1990. However, the weakened ENSO-ISMR relation in the recent period (1991–2020) mostly contributed from the disconnection of La Niña-ISMR relationship compared to El Niño-ISMR, as seen from the large-scale dynamics including the changes in the vertical wind shear and the shift in the Walker circulation. This study highlights how the changes in the patterns and the intensity of the atmospheric as well as oceanic fields within the tropical Indo-Pacific Ocean contributed to the weakening of ENSO-ISMR relation in the recent decades.

1. Introduction

The Indian Summer Monsoon Rainfall (ISMR) from June to September (JJAS) is an essential annual source of precipitation for India, the second most populated county in the world, which has huge influence on the agricultural activities, country’s economy, as well as the life and livelihoods of more than 1.3 billion human population (Webster et al., 1998; Gadgil and Gadgil, 2006; Mishra et al., 2012). Indian Summer Monsoon (ISM) is well known to be a land-atmosphere-ocean coupled system where teleconnections such as the Indian Ocean Dipole, El Niño Southern Oscillation (ENSO), Pacific Decadal Oscillation, North Atlantic Oscillation, Snow cover over Eurasia, Meridional surface air temperature anomaly gradient across Eurasia have the significant influence on the interannual variability of the ISMR (Rasmusson and Carpenter, 1983; Mantua et al., 1997; Saji et al., 1999; Gillett et al., 2003; Kumar et al., 1999; Pai, 2004; Hrudya et al., 2021). Among all, ENSO which is known to be an ocean-atmospheric coupled phenomenon, has been recognized as the most influential drivers of the ISMR interannual variability, since the beginning of the 19th century and which has been greatly explored in many past studies (Walker, 1924; Sikka and Gadgil, 1980; Trenberth, 1997; Webster et al., 1998; Kirtman and Shukla, 2000).

Bjerknes, (1969), pointed out that the influence of ENSO on ISMR is through the interaction between east-west overturning circulation on a vertical plane known as equatorial Walker circulation (Walker, 1923; Walker, 1925) and a north-south overturning circulation called regional Hadley circulation (Halley, 1686; Hadley, 1735). ISMR is well known to have a negative correlation with the simultaneous central-equatorial

Pacific (Niño 3.4 region i.e. area over 5 °S-5 °N and 170 °W-120 °W) Sea Surface Temperature (SST) anomalies, as the development of the La Niña (El Niño) event can enhance (weaken) the ISMR through the displacement of the Walker circulation (Sikka, 1980; Webster and Yang, 1992; Yu et al., 2021). It has been postulated that during warm phase (El Niño) of ENSO, the eastward shift of the Walker cell results in the enhancement of the lower-level convergence over the equatorial Indian ocean, which drives an anomalous Hadley cell with a descending branch over the Indian landmass causing weaker than normal monsoon and below normal rainfall over the Indian subcontinent (Goswami, 1998; Seetha et al., 2020). However, the physical mechanism is still not very much clear because the Indian monsoon is not just affected by the large-scale circulations associated with ENSO but some regional-scale circulations too have their influence.

In many studies, the ISMR-ENSO relationship is observed to have some kind of decadal variations (Kripalani and Kulkarni, 1999; Kumar et al., 1999; Krishnamurthy and Goswami, 2000; Kawamura et al., 2005). However, the reason for this varying relationship is still not very much understood, particularly in the global warming scenario (Cai et al., 2014; Nair et al., 2018). Kumar et al., (1999), hypothesized that the ENSO-ISMR varying relationship could be due to the Eurasian land warming trend. But Pai, (2004), proposed that meridional temperature anomaly gradient over Eurasia is responsible for the ISMR-ENSO relation weakening during 1991–1998. The Indian Ocean Dipole (IOD) is also suggested to have modulating influence on the ISMR-ENSO relationship (Ashok et al., 2004; Ratna et al., 2021; Cherchi et al., 2021). In recent studies, Lu et al., (2006) and Kucharski et al., (2009) showed that the Atlantic Multidecadal Oscillation (AMO) can also play an important role in modifying the ENSO-ISMR relation. Seetha et al., (2020), observed significant variations in the ISMR-ENSO relationship in recent multidecadal epochs, mostly pronounced in the monsoon core zone. They found that, during 1931–1960 (1991–2015), ENSO-ISMR relationship was strong (weak) with correlation value − 0.62 (-0.44) and La Niña (El Niño) was dominating, which gave above (below) normal rainfall over most parts of India. In total contrast, a few studies showed that these interdecadal modulations could be entirely due to stochastic processes or some statistical fluctuations (Gershunov et al., 2001; Van Oldenborgh and Burgers, 2005).

In this study, we intend to investigate the multidecadal variability of the ISMR-ENSO relationship by considering two independent 30-year periods 1961–1990 and 1991–2020. The World Meteorological Organization (WMO) recommends updating the 30-year standard reference periods in every decade to better reflect the changing climate and its influence on our day-to-day weather experience. WMO's Services Commission meeting recommended that the new 30-year baseline 1991–2020, should be adopted globally. In line with the WMO recommendation many countries in the world already switched to the new baseline 1991–2020. So, it is interesting to see how the ISMR-ENSO teleconnection changes in the new baseline period (1991–2020) compared to the earlier independent baseline period(1961–1990). It is also known that the ISMR and ENSO relationship is inconsistent and inhomogeneous, so we tried to focus on the spatial variability over the Indian region. We studied the changes in the SST, circulation patterns and the vertical wind shear in two independent periods for El Niño and La Niña events separately. The paper is organized as follows: Section 2 describes the data used as well as the

methodology applied for the study. Section 3 is dedicated to the results and discussions and finally section 4 summarizes the major findings of this work.

2. Data And Methodology

2.1 Data

NOAA Extended Reconstructed monthly Sea Surface Temperature (ERSST) dataset (Huang et al., 2017) provided by the NOAA PSL, Boulder, Colorado, USA, from their website at https://psl.noaa.gov which is available from January 1854 continuing to the present. Rainfall dataset used for the study is the high spatial resolution (0.25 ° x 0.25 °) gridded monthly rainfall data for the Indian region, from January 1901 to December 2021 by the India Meteorological Department (Pai et al., 2014). For winds and vertical velocity omega, we used monthly mean NCEP-NCAR Reanalysis 1 data (Kalnay et al., 1996) provided by the NOAA PSL, Boulder, Colorado, USA, from their website at https://psl.noaa.gov for the period January 1948 to April 2022. Data for the number of depression days during the monsoon season (JJAS) from 1961–2020, is taken from the India Meteorological Department.

2.2 Methodology

Defining El Niño, La Niña and Neutral Years

To identify the El Niño, La Niña and Neutral Years for the study period, the SST data for the Indian summer monsoon months June, July, August and September (JJAS) are averaged over the Niño 3.4 region in the equatorial Pacific Ocean (5 °N – 5 °S and 120 °W – 170 °W) for the period 1961–2020. The JJAS anomalies are calculated with respect to 1961–2020 climatology. To remove the influence of basin-wide warming because of climate change, we also detrended the SST anomaly. The years are defined as El Niño (La Niña) when the detrended JJAS SST anomalies are greater (smaller) than 0.5 C (-0.5 C), over the Niño 3.4 region. All the remaining years for which the detrended JJAS anomaly values are coming in between – 0.5 C to 0.5 C, are considered as Neutral years.

In order to understand how the relationship between ENSO and ISMR is varying in the recent period as compared to the earlier period, we chose Period 1: 1961–1990 and Period 2: 1991–2020 and all the anomalies are generated with respect to 1961–2020 climatology. To understand the impact of El Niño and La Niña on the Indian landmass, the composite analysis for the El Niño and La Niña events are generated for the two selected periods. The composite anomalies of rainfall, SST, walker circulation, Hadley circulation and vertical wind shear are also analyzed. The statistical significance of the composite analysis is identified based on the Student's t-test.

3. Results And Discussion

3.1 Comparison of ENSO and ISMR during 1961–1990 and 1991–2020

At first, we calculated the number of El Niño and La Niña events during the two independent periods 1961–1990 and 1991–2020 as per the methodology given in Section 2. It was found that there were 5 El Niño events in the period 1961–1990 and it was 7 during the period 1991–2020, which indicates a slight increasing number of El Niño events in the recent decades. Similarly, there were 8 La Niña events during the period 1961–1990 which were slightly decreased to 7 in the recent period 1991–2020.

Next, we checked the mean and standard deviation of JJAS ISMR during the two chosen periods and for El Niño and La Niña events as presented in Fig. 1. The mean JJAS rainfall during 1961–1990 period is 885.76 mm with standard deviation of 97.37 mm, whereas in the 1991–2020 period this amount decreased to 868.79 mm with standard deviation 71.94 mm. The mean JJAS rainfall associated with El Niño events is higher during 1991–2020 period (814.07 mm) compared to 1961–1990 (766.88 mm). It can also be seen from Fig. 1 that the mean JJAS rainfall associated with La Niña is less in the recent 1991–2020 period (904.5 mm) compared to the earlier 1961–1990 period (942.15 mm). The decrease (increase) of the mean JJAS rainfall associated with La Niña (El Niño) years in the recent period compared to earlier period indicates that the ENSO influence over ISMR has weakened in the recent decades as reported in some of the earlier studies (Pai, 2004; Ashok et al., 2019; Hrudya et al., 2021; Seetha et al., 2020). Further analysis with respect to this weakening relationship are discussed in the next section.

3.2 The weakening of the ISMR-ENSO relationship in the recent period

The simultaneous correlation between the JJAS SST anomalies over the Niño 3.4 region and the percentage JJAS rainfall anomalies for the two period are plotted in Figs. 2(a) and 2(b). It was seen that the ISMR-ENSO correlation during 1961–1990 and 1991–2020 periods are − 0.65 and − 0.41 respectively. Also, as seen in the figures, most of above normal rainfall years are associated with La Niña whereas most of the deficient years are associated with El Niño. It was also observed from the figure that the amplitude of the positive seasonal rainfall anomalies associated with La Niña have decreased in the recent period. It can be seen that there were a couple La Niña years 1961–1990 where India received rainfall more than 15% with respect to climatology. However, none of the La Niña years during 1991–2020 exceeds that limit indicates decreasing of La Niña associated rainfall over India in the recent period. Since Indian landmass is large and there are region-wise rainfall variations as well, the spatial distribution of correlation over India was examined for more clarity (Fig. 3). During the period 1961–1990, relatively stronger negative ENSO-ISMR correlations were observed over most parts of India (Fig. 3a). However, during 1991–2020, low correlations were observed over the central core monsoon zone and north-west India (provinces like Punjab, Haryana, Uttarakhand and Himachal Pradesh) indicating weaker ENSO-ISMR relationship (Fig. 3b). At the same time, no significant correlations were observed over the north-east Indian region during both the periods. On the other hand, significant negative correlations were observed over North Indian Jammu-Kashmir-Ladakh region in the earlier period 1961–1990, which has become significantly positive in the recent period 1991–2020. To understand the spatial variation more clearly, the

correlation values between the detrended JJAS SST anomaly over Niño 3.4 region and the percentage rainfall anomaly over the four homogeneous zones of India (as defined by India Meteorological Department) are calculated (Table 1). The correlation over the North-west India and central India was significantly negative during 1961–1990, it has become insignificant in the recent period 1991–2020. Correlation value over North-East India was insignificant during both the periods whereas, over the peninsular India negative significant correlation was observed during both the periods.

Table 1
Correlation between % rainfall anomaly (JJAS) and detrended Niño3.4 SST anomaly (JJAS) over the four homogeneous zones of India during the two periods.

	1961–1990	1991–2020
North-West India	-0.71*	-0.34
Central India	-0.51*	-0.20
North-East India	-0.17	-0.13
South Peninsular India	-0.58*	-0.42*
All India	-0.65*	-0.41*
*Statistically significant correlation values with 95% confidence level.		

We next analyzed the JJAS composite rainfall anomaly patterns over the Indian region corresponding to the El Niño and La Niña years for the two periods and shown in Fig. 4. The El Niño composite rainfall anomalies during 1961–1990 (Fig. 4a) show large negative values (≤ -35 mm month ^{1}) over many areas of North-West India, and provinces like Uttarakhand, Himachal Pradesh, Punjab, Rajasthan, central India including Madhya Pradesh, Gujarat and Maharashtra. However, positive rainfall anomalies are observed over most parts of the North-East region, some areas of provinces like Bihar and Jharkhand. This figure indicates that the El Niño composite rainfall anomalies during the period 1991–2020 (Fig. 4c) are weaker in many parts of India than that of 1961–1990. In the La Niña composite during 1961–1990 (Fig. 4b), most parts of Indian landmass had positive JJAS rainfall anomalies except a few regions of provinces like Odisha, Gujarat and Jammu-Kashmir. However, during the period 1991–2020 (Fig. 4d), JJAS rainfall anomaly become negative in almost all over the central India and core monsoon zone in the provinces like Chhattisgarh, Madhya Pradesh, Uttar Pradesh, Rajasthan, and weak positive rainfall anomaly values are observed over the parts of northern and western and peninsular India as compared to the previous period. The JJAS rainfall anomaly clearly indicates that the El Niño associated-deficient monsoon rainfall and La Niña associated excess monsoon rainfall, both were weakening its intensity over most parts of the Indian region in the recent decades.

3.3 Mechanisms contributing to the weakening of the ISMR-ENSO relationship in the recent period

To identify the factors contributing to the difference in the El Niño and La Niña composite rainfall anomalies between the two periods considered here, corresponding SST anomalies and various circulation anomalies were examined. Figure 5 shows the composite of detrended JJAS SST anomalies over the tropical regions of Pacific and Indian ocean corresponding to the El Niño and La Niña years for the period 1961–1990 and 1991–2020. In the case of El Niño SST composites (Fig. 5a and 5c), the spread of warm temperature anomalies over the eastern and central Pacific region were narrow in the recent 1991–2020 period compared to 1961–1990. The La Niña composite during 1961–1990 (Fig. 5b) shows a clear cold tongue signature pattern with significant negative SST anomalies extending from the central to the eastern Pacific Ocean. On the other hand, during 1991–2020, relatively weaker cold SST anomalies were observed over the central Pacific Ocean and no significant SST anomalies were observed over the far eastern Pacific Ocean (Fig. 5d).

To understand the mechanisms behind such rainfall variation during different composites, velocity potential along with the divergent wind vectors were analyzed at upper level (200 hPa) for the earlier period 1961–1990 and recent period 1991–2020 considering El Niño and La Niña composite anomaly (Fig. 6). During 1961–1990, El Niño composite shows divergence over the central Pacific region and the convergence over the Maritime continent as well as the Indian ocean including the Indian landmass (Fig. 6a). The convergence and the divergence, both are found to be shifted eastward indicating the eastward shift in the Walker circulation with a reduction in its strength during the recent period (Fig. 6c). La Niña composite in the period 1961–1990, shows the divergence over the western and central western Pacific (Fig. 6b) which has shifted further westward over the western Indian ocean in the recent period 1991–2020 with a major reduction in the strength of the divergence (Fig. 6d). The upper-level convergence during La Niña is more confined to the eastern Pacific during the 1961–1990 period but the westward shift in the convergence was observed over the east and central eastern Pacific in the recent period 1991–2020.

To understand the ENSO associated circulation better and how it is influencing the Indian monsoon systems, we have further analyzed the Walker and Hadley circulations. The typical explanation of the ENSO-induced teleconnection response in the Indian Monsoon is normally analyzed via the large-scale east-west shift in the tropical Walker circulation. During an El Niño event, the rising limb of the Walker circulation and the associated tropical convection observed over the anomalously warm waters in the eastern and central Pacific (Kumar et al., 1999). As a consequence of this, an anomalous subsidence is generally found extending from the western Pacific and the Indian subcontinent. It is linked with anomalously low pressure over the central and eastern Pacific and anomalously high pressure over the western Pacific and eastern Indian ocean. Sir Gilbert Walker first noticed that these pressure oscillations can influence the rainfall and monsoon circulation over the Indian region up to a large extent (Walker, 1918). Later, many other observational studies also noted this connection (Rasmusson and Carpenter, 1983, Ropelewski and Halpert, 1987).

In order to understand the contribution that the Pacific Ocean wind pattern may make to the rainfall variability over the Indian landmass, we compared the east-west Walker circulation patterns over the Indo-

Pacific region, for the two chosen periods during El Niño and La Niña events (Fig. 7). During the 1961–1991 El Niño composite (Fig. 7a), strong ascending motion (convection) can be seen in the central Pacific region whereas descending motion (subsidence) over the west Pacific and over the Indian region (60 E to 120 E). But the strength of descending motion over the Indian ocean fairly reduced in the recent period 1991–2020 (Fig. 7c). During the La Niña composites in the two periods (Fig. 7b and Fig. 7d), fairly widespread ascending motion (convection) was observed over the Indian region which has weakened so much in the recent period 1991–2020.

It was earlier found that the Walker circulation and the tropical north-south Hadley circulation are associated with ENSO (Power and Smith, 2007, Stachnik and Schumacher, 2011, Hrudya et al., 2021). The regional Hadley circulation over the Indian landmass is recognized as a meridional overturning circulation in which the hot air rises at the equatorial region and moves pole-ward, when cools, it sinks and moves back towards the equator. This coupled air-sea feedback over the Indian Ocean is suggested to modify the meridional overturning circulation during the ENSO phases, which affects the ISMR (Wu and Kirtman, 2004). The analysis of Hadley circulation indicates that during 1961–1990 El Niño composite (Fig. 8a), strong descending motion (subsidence) can be seen around 20 N to 35 N (JJAS rainfall anomaly plot for this period was showing strong negative rainfall anomaly in Fig. 4a) at the same time, there is no strong ascending or descending motion present from 0 to 20 N. But both the ascending and descending motions can be clearly observed all across the Indian landmass in the period 1991–2020 (Fig. 8c). During the La Niña events in the period 1961–1990 (Fig. 8b), a strong ascending motion (convection) is observed over the almost entire Indian landmass (from 10 N up to 33 N) which contributed to the above normal rainfall across the entire Indian region (Fig. 4b). However, the presence of ascending motion is found to be fairly reduced in the recent period 1991–2020 and the subsidence was seen over the central and northern Indian region (from 20 N to 30 N) (Fig. 8d). This is one of the reasons for the less rainfall over central and northern regions during 1991–2020 La Niña compared to 1961–1990. It was also seen that in the recent 1991–2020 period La Niña, rising motion is prominent over the southern peninsular India (0 to 10 N) which contributed to strong positive rainfall anomaly over this region (Fig. 4d) in the recent period.

As the vertical wind shear plays a very important role in the convection and the production of rainfall over India (Ratna et al., 2020), we have used the conventional method to calculate the vertical wind shear of the zonal wind component over the Indian subcontinent as the difference between the zonal winds at lower-level (850 hPa) and upper-level (200 hPa). Vertical wind shear anomaly composites for El Niño and La Niña in the two considered periods are plotted in Fig. 9. Strong positive value (3.406 m s ^{1}) of vertical wind shear anomaly is observed during 1961–1990 La Niña composite, which has reduced so much (-0.794 m s ^{1}) in the 1991–2020 period coincides with reduction of rainfall over Indian region. A recent study conducted by Samanta et al., 2020 also highlighted that according to the Atmospheric General Circulation Model (AGCM) more than 50% of the ISMR reduction during post 1980 La Niña episodes is only due to the weakening of the La Niña strength as well as the pattern. During 1961–1990, the vertical wind shear anomaly composite during El Niño, showed strong negative value (-4.139 m s ^{1}), this is also found to be weakened (-3.355 m s ^{1}) in the recent 1991–2020 period coincides with reduction of negative

rainfall anomaly strength in the recent decades. Clearly the decrease in the magnitude of vertical wind shear anomaly value is more in case of La Niña compared to El Niño. This indicates that the La Niña associated rainfall played a major role to weaken the ENSO-ISMR teleconnection compared to El Niño associated rainfall.

4. Summary And Conclusions

In the present study, the modulation of ENSO-ISMR interlinkage was examined in the recent decades by analyzing rainfall, SST and atmospheric circulation for two independent climatological periods of 1961–1990 and 1991–2020. In line with the WMO recommendation many countries in the world switched to the new baseline 1991–2020 to discuss the climate normal. So, effort was made to see how the ISMR-ENSO teleconnection changed in the new baseline period (1991–2020) compared to the earlier independent baseline period (1961–1991). It was observed that the ENSO-ISMR teleconnection has weakened in the recent period (1991–2020) compared to the earlier period (1961–1990) where the correlation between ENSO and ISMR has reduced from − 0.65 to -0.41. The relationship between ENSO teleconnection and rainfall for four homogeneous regions also indicates decreased correlation except for south peninsular India. It was seen that 4 out of 5 El Niño years were having below normal rainfall in the early period 1961–1990. However, in the recent period 1991–2020, only 3 out of 7 El Niño years were having below normal rainfall during the monsoon season over the Indian region. It was also seen that there were a couple of La Niña years during the period 1961–1990 where ISMR anomaly was more than 15% with respect to climatology. However, none of the La Niña years during the 1991–2020 period reached that limit. From this observational analysis, we confirmed that during the recent 1991–2020 La Niña period, there is a significant reduction in the monsoon rainfall over the central core monsoon region as well as over the north-west Indo-Gangetic area, which is the major agricultural production region of India. We found that the El Niño associated-deficient monsoon rainfall and La Niña associated excess monsoon rainfall over India, both were reducing its intensity in the recent decades over most parts of the Indian region. These changing patterns of rainfall during El Niño as well as La Niña can be associated with the changes in the SST in the tropical Pacific Ocean and associated large scale dynamics. Generally, La Niña supports the excess ISMR by strengthening the Walker Circulation pattern but our analysis showed that during La Niña composite, there is a westward shift in the Walker Circulation during 1991–2020, due to which the rising motion pattern was shifted further westward in the recent period contributed to the reduction in La Niña associated rainfall over Indian region. However, during El Niño composite, an eastward shift in the Walker Circulation was observed in the 1991–2020 period and contributed to more rainfall over Indian region compared to the earlier 1961–1990 period. It was also observed that the magnitude of vertical wind shear anomaly has decreased its intensity in case of El Niño as well as La Niña. However, reduction in the magnitude was found to be more in the case of La Niña composite as compared to the El Niño composite. This indicates that the weakening of La Niña associated above normal rainfall has contributed more to the weak ENSO-ISMR teleconnection, compared to the El Niño associated below normal rainfall in the recent period.

While so many recent studies focused on the connection between El Niño and warming trends, we made an attempt to study the El Niño-below normal ISMR and La Niña-above normal ISMR relationship, as both are equally important in order to understand the complete ENSO phenomenon. Definitely, various potential factors and teleconnections other than ENSO (for example Indian Ocean Dipole, Atlantic Multidecadal Oscillation, Equatorial Indian Ocean Oscillation, Eurasian snow cover to name a few) are also affecting ISMR (Kumar et al., 1999; Gadgil et al., 2007; Cherchi et. al. 2021, Hrudya et. al., 2020, Ratna et. al., 2021) but how they changed in the recent period are beyond the scope of this study. Few recent studies discussed that the low frequency modulation in the relationship between any two climate variables may appear periodic or merely a stochastic process (Gershunov et al., 2001; Samanta et al., 2020) but the analysis in this paper gives us opportunity to understand the major change in large-scale dynamics that influence such relationship between ENSO and ISMR

Declarations

Statements and Declarations

Funding

The authors declare that no funds, grants, or other support were received during the preparation of this manuscript.

Competing Interests

The authors have no competing interests to declare that are relevant to the content of this article.

Author Contributions

All authors contributed to the study conception and design. Material preparation, data collection and analysis were performed by Tanu Sharma with support from Satyaban B Ratna and D. S. Pai. The first draft of the manuscript was written by Tanu Sharma and all authors commented on previous versions of the manuscript. All authors read and approved the final manuscript.

Data Availability

NOAA Extended Reconstructed monthly Sea Surface Temperature (ERSST) dataset (Huang et al., 2017) provided by the NOAA PSL, Boulder, Colorado, USA fromJanuary 1854 continuing to the present available at *https://psl.noaa.gov*. High spatial resolution (0.25 ° x 0.25 °) gridded monthly rainfall dataset from India Meteorological Department (Pai et al., 2014) used for the study from January 1901 to December 2021 available at https://www.imdpune.gov.in/cmpg/Griddata/Rainfall_25_NetCDF.html. For winds and vertical velocity, monthly mean NCEP-NCAR Reanalysis 1 data (Kalnay et al., 1996) provided by the NOAA PSL, Boulder, Colorado, USA, from their website at *https://psl.noaa.gov* for the period January 1948 to April 2022.

References

1. Ashok, K., Guan, Z., Saji, N. H., and Yamagata, T. (2004). Individual and combined influences of ENSO and the Indian Ocean dipole on the Indian summer monsoon. *J Clim*, *17*, 3141–3155.
2. Ashok, K., Feba, F., and Tejavath, C. T. (2019). The Indian summer monsoon rainfall and ENSO. *Mausam, 70, 3*, 443-452.
3. Bjerknes, J. (1969). Atmospheric teleconnections from the equatorial Pacific. *Monthly Weather Rev*, *97*, 163–172.
4. Cai, W., Borlace, S., Lengaigne, M., Rensch, P. V., Collins, M., Vecchi, G., Timmermann, A., Santoso, A., McPhaden, M. J., Wu, L., England, M. H., Wang, G., Guilyardi, E., and Jin, F. F. (2014). Increasing frequency of extreme El Niño events due to greenhouse warming. *Nat Clim Change*, *4*, 111–116. https://doi.org/10.1038/nclimate2100
5. Cherchi, A., Terray, P., Ratna, S. B., Sankar, S., Sooraj, K. P., and Behera, S. (2021). Chapter 8 - Indian Ocean Dipole influence on Indian summer monsoon and ENSO: A review, Indian Summer Monsoon Variability. *Elsevier*, *ISBN 9780128224021*, 157-182. https://doi.org/10.1016/B978-0-12-822402-1.00011-9.
6. Gadgil, S., and Gadgil, S. (2006). The Indian monsoon, GDP and agriculture. *Econ Political Wkly*, *41*, 4887–4895.
7. Gadgil S., Rajeevan M. and Francis P A (2007) *Monsoon variability: links to major oscillations over the equatorial Pacific and Indian oceans* Curr. Sci. 93 182–94.
8. Gershunov, A., Schneider, N., and Barnett, T. (2001). Low–frequency modulation of the ENSO–Indian monsoon rainfall relationship: signal or noise? *J Clim*, *14*, 2486–2492. https://doi.org/10.1175/1520-0442(2001)014<2486:LFMOTE>2.0.CO;2
9. Gillett, N. P., Graf, H. F., and Osborn, T. J. (2003). Climate change and the North Atlantic oscillation. *Geophys Monogr Am Geophys Union*, *134*, 193–210.
10. Goswami, B. N. (1998). Interannual variations of Indian summer monsoon in a GCM: external conditions versus internal feedbacks. *J Clim*, *11*, 501–522. 10.1175/1520-0442(1998)011<0501:IVOISM>2.0.CO;2
11. Goswami B. N. and Mohan R. S. (2000). Intraseasonal Oscillations and Interannual variability of the Indian Summer Monsoon. *Journal of Climate,* vol 14, 1180-1198.
12. Hadley, G. (1735). IV Concerning the cause of the general trade–winds. *Philoso Trans R Soc Lond*, *39*, 58–62.
13. Halley, E. (1686). An historical account of the trade winds, and monsoons, observable in the seas between and near the tropics, with an attempt to assign the physical cause of the saID winds. *Philos Trans R Soc Lond*, *16*, 153–168.
14. Hrudya, P. H., Varikoden, H., and Vishnu, R. (2021). A review on the Indian summer monsoon rainfall, variability and its association with ENSO and IOD. *Meteorology and Atmospheric Physics*, *133*, 1-14. https://doi.org/10.1007/s00703-020-00734-5.

15. Huang, B., Peter W. Thorne, et. al, (2017). Extended Reconstructed Sea Surface Temperature version 5 (ERSSTv5), Upgrades, validations, and intercomparisons. *J. Climate*, doi: 10.1175/JCLI-D-16-0836.1
16. Kalnay E, Kanamitsu M, Kistler R, Collins W, Deaven D, Gandin L, Iredell M, Saha S, White G, Woollen J, Zhu Y (1996). The NCEP/NCAR 40–issued reanalysis project. *Bull Am Meteorol Soc,* 77, 437–472 https://doi.org/10.1175/1520-0477(1996)077<0437:TNYRP>2.0.CO;2
17. Kawamura, R., Uemura, K., and Suppiah, R. (2005). On the recent change of the Indian summer monsoon-ENSO relationship. *SOLA*, *1*, 201-204. 10.2151/sola.2005-052
18. Kirtman, B., and Shukla, J. (2000). Influence of the Indian summer monsoon on ENSO. *Quart. J. Roy. Meteor. Soc*, *126*, 213–239. 10.1002/qj.49712656211
19. Kripalani, R. H., and Kulkarni, A. (1999). Climatology and variability of historical Soviet snow depth data: some new perspectives in snow— Indian monsoon teleconnections. *Clim Dyn*, *15*, 475–489.
20. Krishnamurthy, V., and Goswami, B. N. (2000). Indian monsoon–ENSO relationship on interdecadal timescale. *J Clim*, *13*, 579–595.
21. Kucharski, F., Bracco, A., Yoo, J. H., Tompkins, A. M., Feudale, L., Ruti, P., and Dell'Aquila, A. (2009). A Gill–Matsuno type mechanism explains the tropical Atlantic influence on African and Indian monsoon rainfall. *Q J R Meteorol Soc*, *135*, 569–579. 10.1002/qj.406
22. Kumar, K. K., Rajagopalan, B., and Cane, M. A. (1999). On the Weakening Relationship Between the Indian Monsoon and ENSO. *Science*, *284*(5423), 2156-2159. 10.1126/science.284.5423.2156
23. Lu, R., Dong, B., and Ding, H. (2006). Impact of the Atlantic multidecadal oscillation on the Asian summer monsoon. *Geophy Res Lett*, *33*, L24701. 10.1029/2006GL027655
24. Mandke S, Sahai A K, Shinde M A, Susmitha Joseph and Chattopadhyay R 2007 Simulated changes in active/break spells during the Indian summer monsoon due to enhanced CO2 concentrations: Assessment from selected coupled atmosphere–ocean global climate models; Int. J. Climatol. 27 837–859.
25. Mantua, N. J., Hare, S. R., Zhang, Y., Wallace, J. M., and Francis, R. C. (1997). A Pacific interdecadal climate oscillation with impacts on salmon production. *Bull Am Meteorol Soc*, *78*, 1069–1080.
26. Mishra, V., Smoliak, B. V., and Lettenmaier, D. P. (2012). A prominent pattern of year-to-year variability in Indian summer monsoon rainfall. *P. Natl. Acad. Sci. USA.*, *109*, 7213–7217.
27. Nair, P. J., Chakraborty, A., Varikoden, H., Francis, P. A., and Kuttippurath, J. (2018). The local and global climate forcings induced inhomogeneity of Indian rainfall. *Sci Rep*, *8*, 6026.
28. Pai, D. S. (2004). A Possible mechanism for the weakening of El Nino-monsoon relationship during the recent decade. *Meteorol Atmos Phys*, *86*, 143-157. 10.1007/s00703-003-0608-8
29. Pai, D.S., Latha Sridhar, Rajeevan M., Sreejith O.P., Satbhai N.S. and Mukhopadhyay B., (2014). Development of a new high spatial resolution (0.25° X 0.25°) Long period (1901-2010) daily gridded rainfall data set over India and its comparison with existing data sets over the region. *MAUSAM, 65, 1*, 1-18.

30. Power, S. B., and Smith, I. N. (2007). Weakening of the Walker Circulation and apparent dominance of El Niño both reach record levels, but has ENSO really changed? *Geophys Res Lett*, *34:L18702*. 10.1029/2007GL030854
31. Rajeevan M., Gadgil S., and Bhate J. (2010). Active and break spells of the Indian summer_monsoon. *J. Earth Syst. Sci.* 119, No.3, 229-247.
32. Rasmusson, E. M., and Carpenter, T. H. (1983). The Relationship Between Eastern Equatorial Pacific Sea Surface Temperatures and Rainfall over India and Sri Lanka. *Monthly Weather Review*, *111*, 517-528.
33. Ratna, S. B., Cherchi, A., Osborn, T. J., Joshi, M., and Uppara, U. (2021). The Extreme Positive Indian Ocean Dipole of 2019 and Associated Indian Summer Monsoon Rainfall Response. *Geophy. Res. Lett.*, *48*, 1-11. 10.1029/2020GL091497
34. Ratna, S. B., T. J. Osborn, M. Joshi, and J. Luterbacher (2020). The influence of Atlantic variability on Asian summer climate is sensitive to the pattern of the sea surface temperature anomaly, Journal of Climate, 33, 17, 7567-7590. https://doi.org/10.1175/JCLI-D-20-0039.1
35. Ropelewski, C. F., and Halpert, M. S. (1987). Global and Regional Scale Precipitation Patterns Associated with the El Niño/Southern Oscillation. *Monthly Weather Review*, *115*, 1606-1626. https://doi.org/10.1175/1520-0493(1987)115<1606:GARSPP>2.0.CO;2
36. Saji, N. H., Goswami, B. N., Vinayachandran, P. N., and Yamagata, T. (1999). A dipole mode in the tropical Indian Ocean. *Nature*, *401*, 360-363.
37. Samanta, D., Rajagopalan, B., Karnauskas, K. B., Zhang, L., and Goodkin, N. F. (2020). La Niña's Diminishing Fingerprint on the Central Indian Summer Monsoon. *Geophy. Res. Lett.*, *47*, 1-11. 10.1029/2019GL086237
38. Seetha, C. J., Varikoden, H., Babu, C. A., and Kuttippurath, J. (2020). Significant changes in the ENSO-monsoon relationship and associated circulation features on multidecadal timescale. *Climate Dynamics*, *54*, 1491–1506. https://doi.org/10.1007/s00382-019-05071-x
39. Sikka, D. R. (1980). Some aspects of the large scale fluctuations of summer monsoon rainfall over India in relation to fluctuations in the planetary and regional scale circulation parameters. *Proceedings of the Indian Academy of Sciences - Earth and Planetary Sciences*, *89(2)*, 179–195. https://doi.org/10.1007/BF02913749
40. Sikka, D. R., and Gadgil, S. (1980). On the maximum cloud zone and the ITCZ over Indian, longitudes during the southwest monsoon. *Mon Weather Rev*, *108*, 1840–1853.
41. Stachnik, J. P., and Schumacher, C. (2011). A comparison of the Hadley circulation in modern reanalysis. *Geophysical Research Letter*, *116:D22102*. https ://doi.org/10.1029/2011JD016677
42. Trenberth, K. E. (1997). The definition of El Niño. *Bull Am Meteor Soc*, *78*, 2771–2778.
43. Van Oldenborgh, G. J., and Burgers, G. (2005). Searching for decadal variations in ENSO precipitation teleconnections. *Geophys Res Lett*, *32*, L15701. https://doi.org/10.1029/2005GL023110
44. Walker, G. T. (1918). Correlation in seasonal variation of weather. *Q.J.R.Meteorol.Soc.*, *44*, 223-224.

45. Walker, G. T. (1923). Correlation in seasonal variation of weather. VIII: a preliminary study of world weather. *Mem India Meteorol Dept*, *24*, 75–131.
46. Walker, G. T. (1924). Correlation in seasonal variations of weather—a further study of world weather. *Mon. Weather Rev*. :10.1175/1520-0493(1925)53
47. Walker, G. T. (1925). Correlation in seasonal variations of weather—a further study of world weather. *Mon Weather Rev*, *53*, 252–254.
48. Webster, P. J., Magana, V., Palmer, T. N., Shukla, J., Tomas, R. A., and Yanai, M. (1998). Monsoons: processes, predictability and the prospects for prediction. *J. Geophys. Res*, *103*, 14451–14510. 10.1029/97JC02719
49. Webster, P. J., Magana, V. O., Palmer, T. N., Shukla, J., Tomas, R. A., Yanai, M. U., and Yasunari, T. (1998). Monsoons: processes, predictability, and the prospects for prediction. *J Geophys Res*, *103*, 14451–14510.
50. Webster, P. J., and Yang, S. (1992). Monsoon and ENSO: Selectively interactive systems. *Quarterly Journal of the Royal Meteorological Society*, *118(507)*, 877–926. https://doi.org/10.1002/qj.49711850705
51. Wu, R., and Kirtman, B. P. (2004). Impacts of the Indian Ocean on the Indian summer monsoon – ENSO relationship. *J Clim*, *17*, 3037–3054.
52. Yu, S. Y., Fan, L., Zhang, Y., Zheng, X. T., and Li, Z. (2021). Reexamining the Indian Summer Monsoon Rainfall– ENSO relationship from its recovery in the 21st century: Role of the Indian Ocean SST anomaly associated with types of ENSO evolution. *Geophysical Research Letters*, *48*. e2021GL092873

Figures

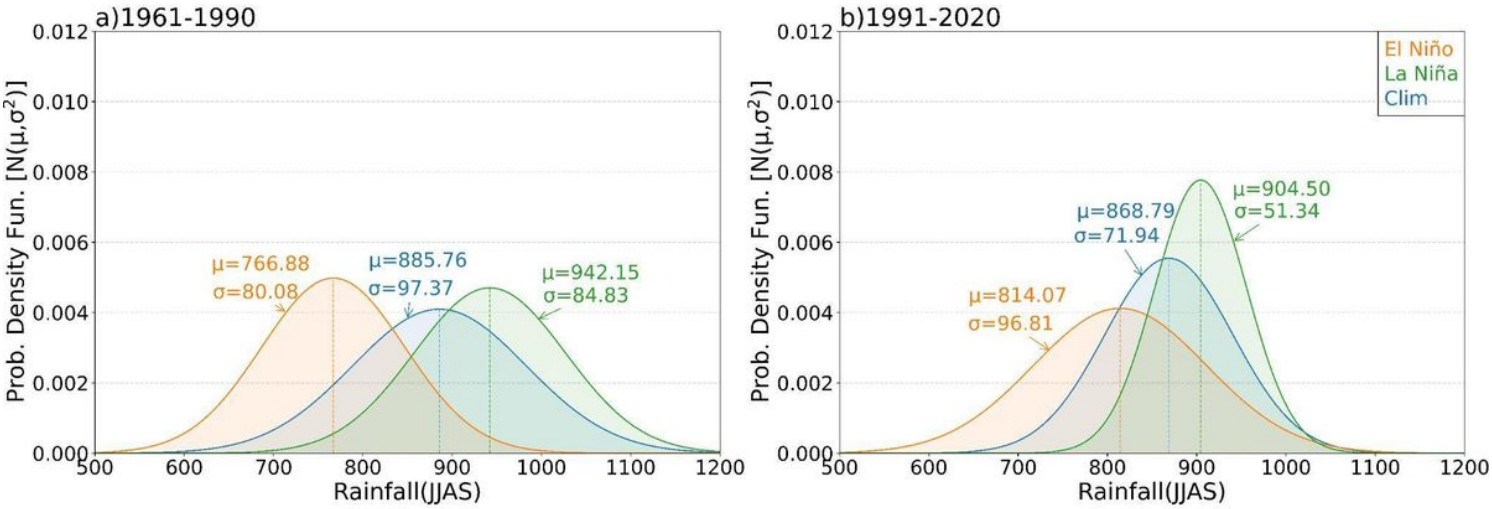

Figure 1

Normal distribution curve representing the mean (μ) and standard deviation (σ) of the JJAS ISMR (mm) for the composite of El Niño, La Niña and mean Climatology for the period **(a)** 1961-1990 and **(b)** 1991-2020.

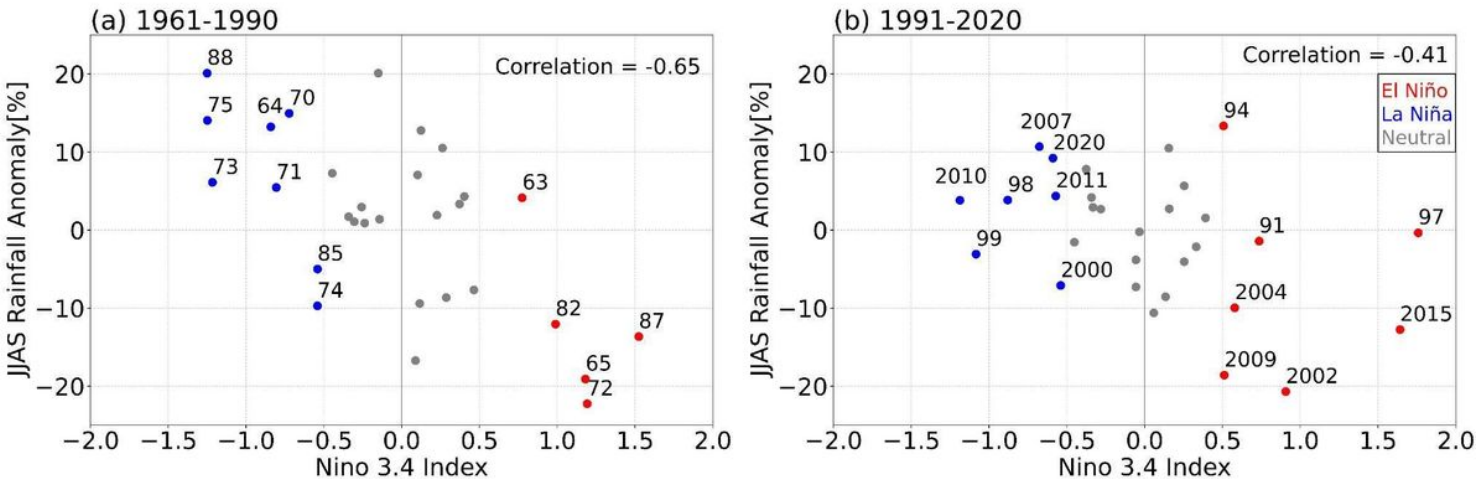

Figure 2

Simultaneous correlation between JJAS percentage rainfall anomaly and JJAS detrended Niño3.4 SST anomaly for the period **(a)** 1961-1990 and **(b)** 1991-2020.

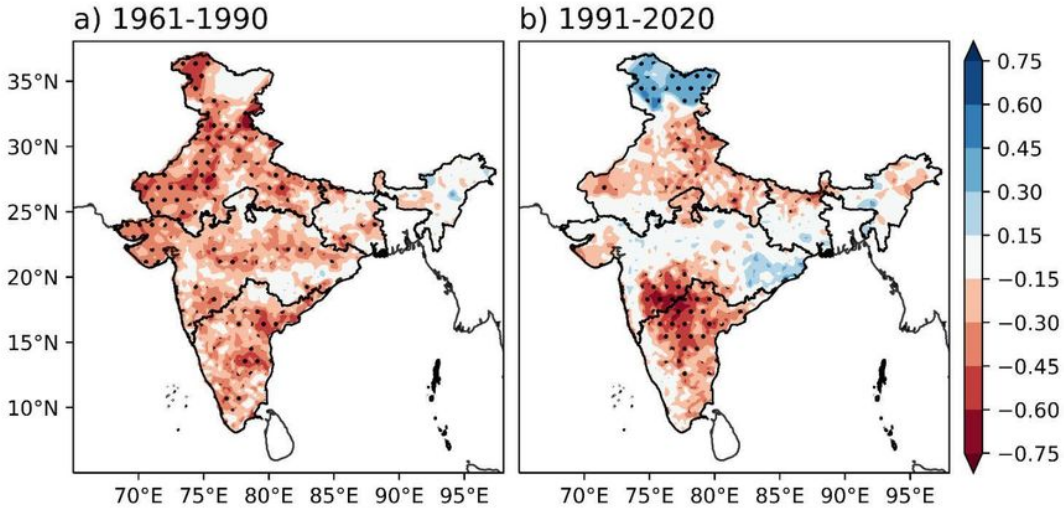

Figure 3

Simultaneous correlation between JJAS detrended SST anomaly over Niño 3.4 region (5 N-5 S, 120 W-170 W) and JJAS rainfall anomaly over India for **(a)** 1961-1990 and **(b)** 1991-2020. Dotted areas

representing significant at 90 % confidence level based on two-tailed Student's t-test.

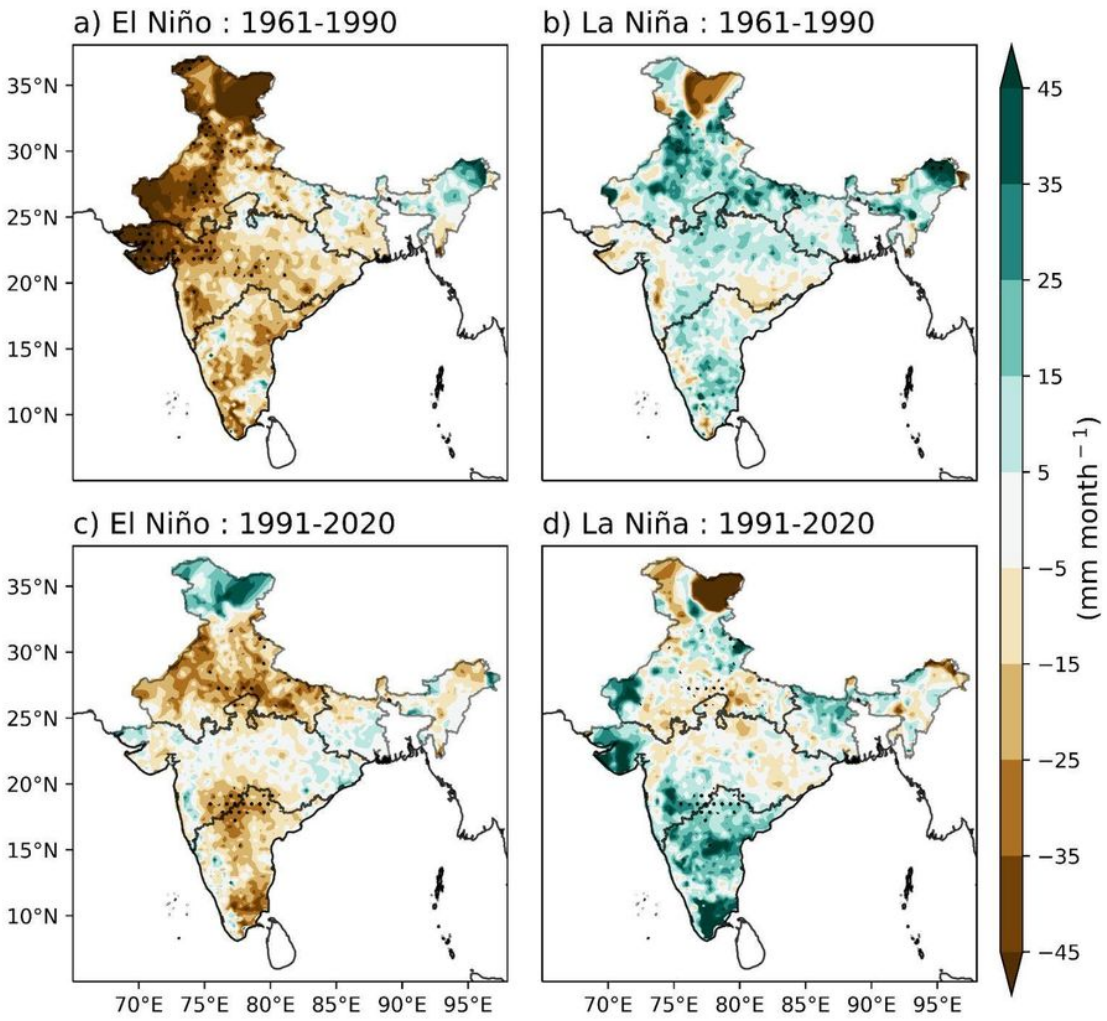

Figure 4

Composites of June-September (JJAS) rainfall anomaly (in mm month ^{1}) for **(a)** El Niño and **(b)** La Niña during the period 1961-1990. **(c)** and **(d)** are the same as (a) and (b), but for the period 1991-2020. Dotted areas representing significant anomaly values at 90 % confidence level based on two-tailed Student's t-test.

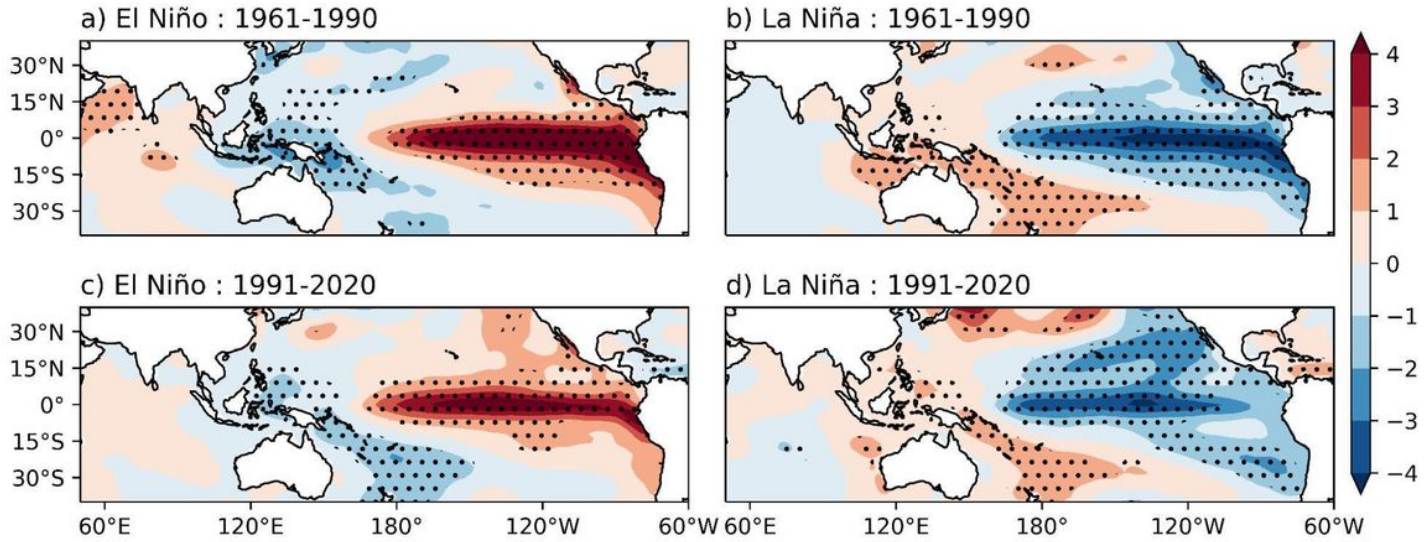

Figure 5

Composites of June-September (JJAS) detrended Sea Surface Temperature Anomaly (in C) for **(a)** El Niño and **(b)** La Niña during the period 1961-1990. **(c)** and **(d)** are the same as (a) and (b), but for the period 1991-2020. Anomaly values are calculated from 1961-2020 climatology. Dotted areas representing significant anomaly values at 90 % confidence level based on two-tailed Student's t-test.

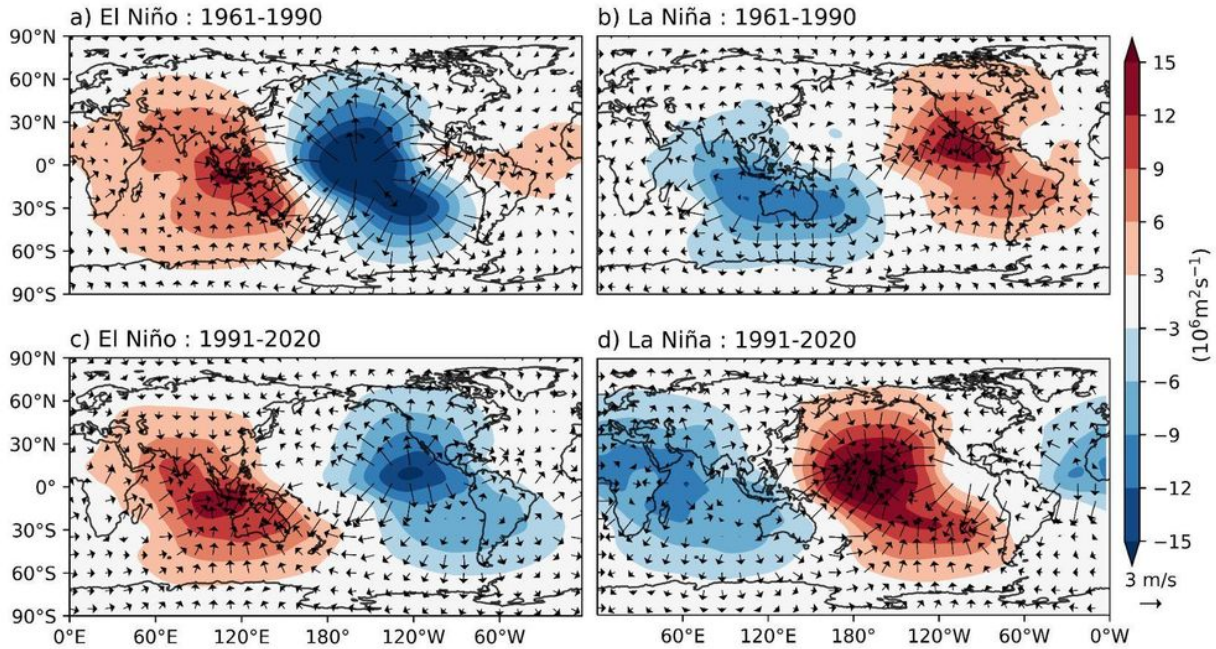

Figure 6

Velocity Potential Anomaly Composite (shaded, 10 m² s ¹) along with the divergent wind (vector) is plotted at 200 hPa for **(a)**El Niño and **(b)** La Niña during the period 1961-1990. **(c)** and **(d)** are the same as (a) and (b), but for the period 1991-2020.

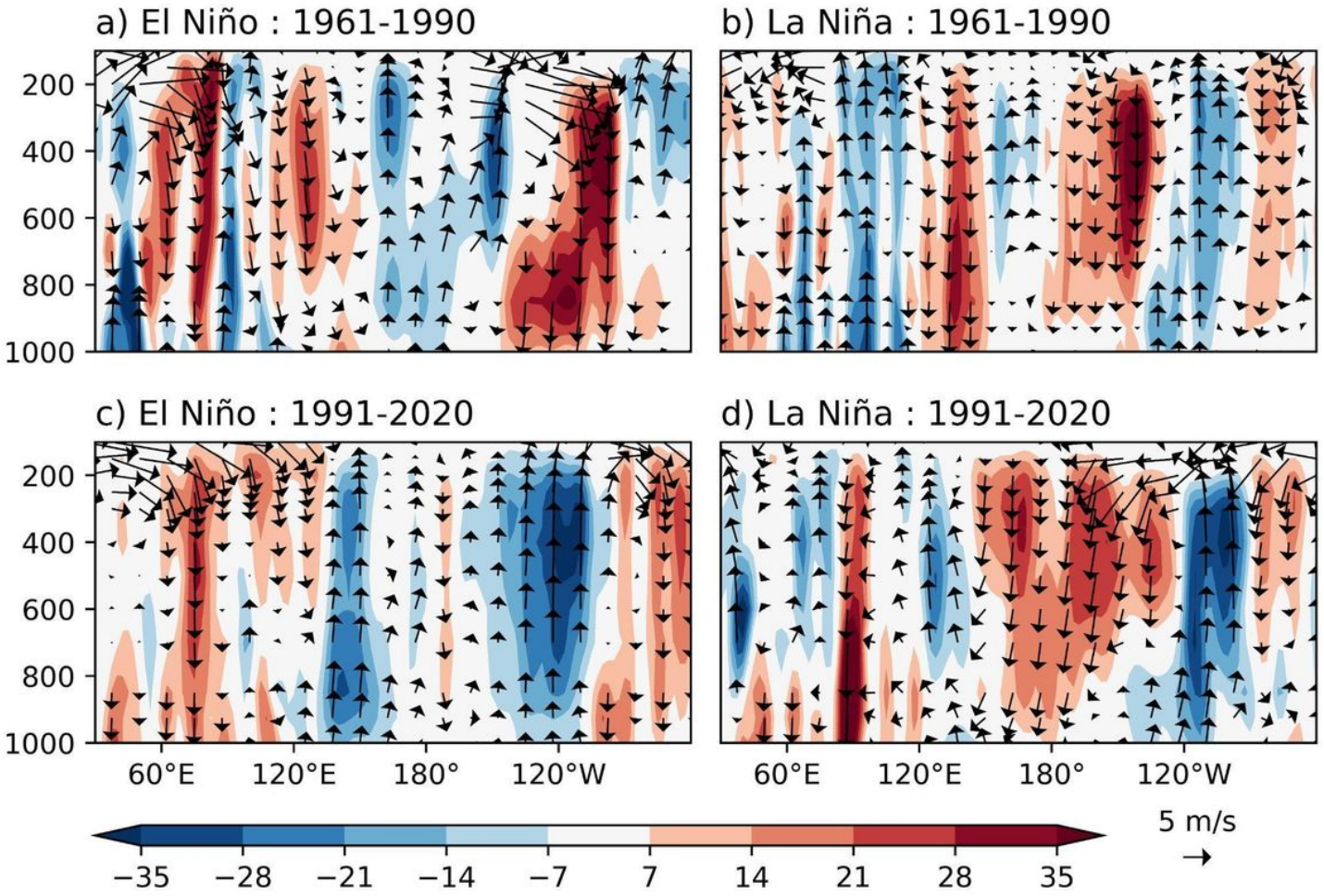

Figure 7

Walker circulation anomalies over the Indo-Pacific sector for **(a)**El Niño and **(b)** La Niña during the period 1961-1990. **(c)** and **(d)** are the same as (a) and (b), but for the period 1991-2020. Vector plotted using zonal (u) and vertical (w) wind, from 1000 hPa to 100 hPa. Values averaged over latitude 7.5 N - 37.5 N. Color contour representing w 10³ m s ¹.

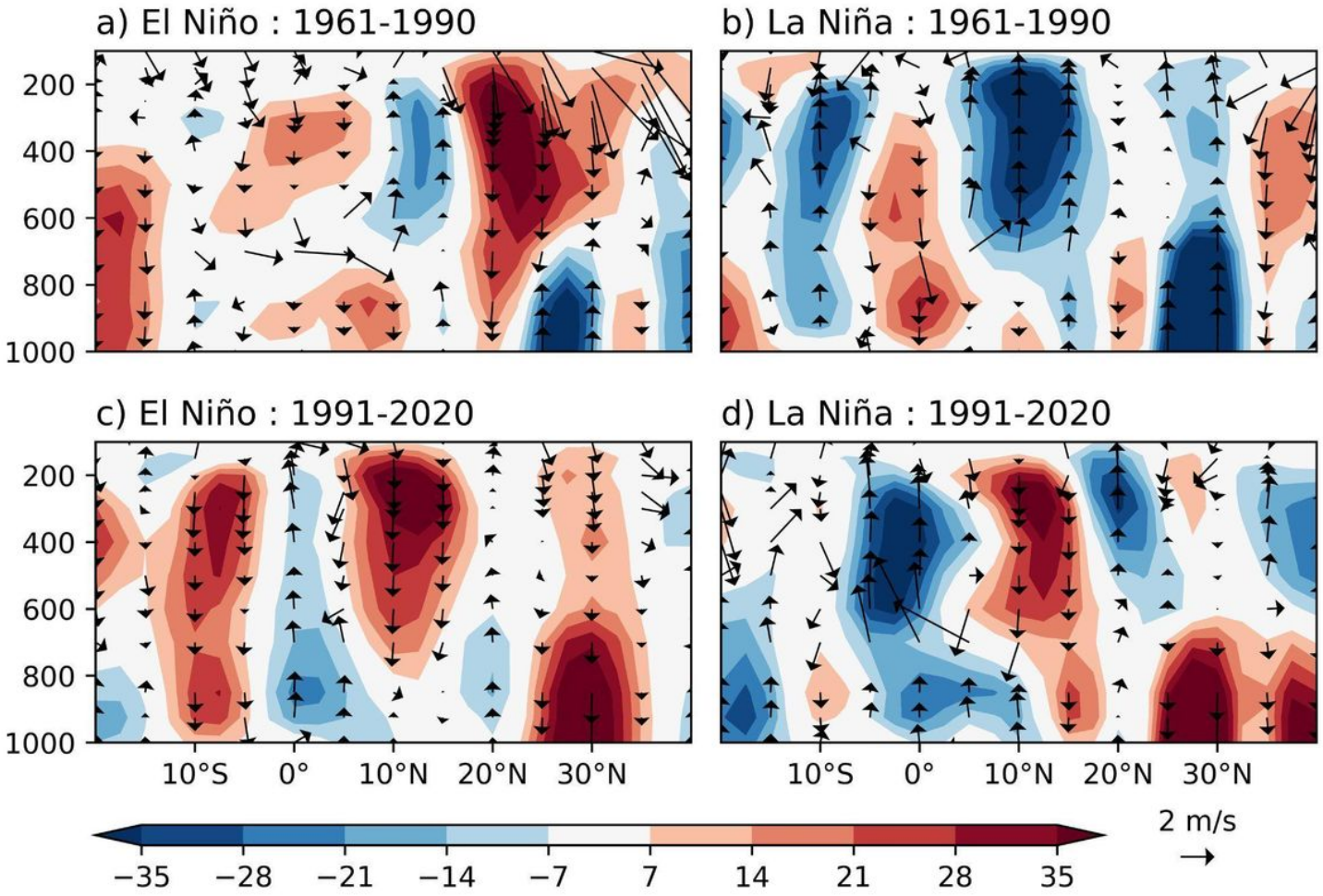

Figure 8

Hadley circulation anomalies over the Indian ocean and landmass for **(a)** El Niño and **(b)** La Niña during the period 1961-1990. **(c)**and **(d)** are the same as (a) and (b), but for the period 1991-2020. Vector plotted using meridional (v) and vertical (w) wind, from 1000 hPa to 100 hPa. Values averaged over longitude 67.5 E - 97.5 E. Color contour representing w 10^3 m s^{-1}.

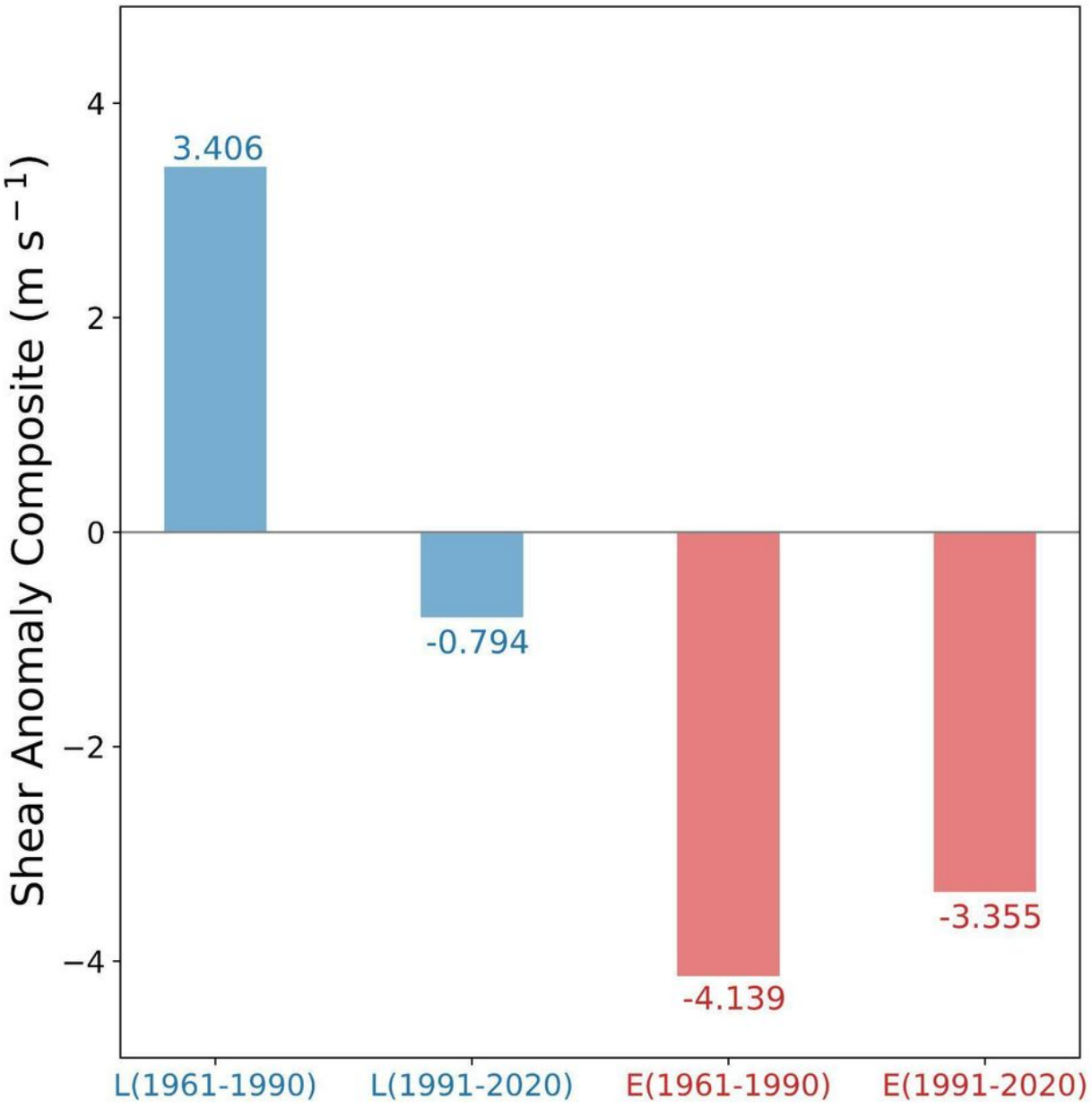

Figure 9

Vertical wind shear of the zonal wind component (u) values for the JJAS period are averaged spatially over the Indian region (7.5 N - 37.5 N and 67.5 E - 97.5 E). Anomaly values are plotted for the **L(1961-1990)** (La Niña 1961-1990 composite), **L(1991-2020)** (La Niña 1991-2020 composite), **E(1961-1990)**(El Niño 1961-1990 composite) and **E(1991-2020)**(El Niño 1991-2020 composite).